African Journal of Pure & Applied Sciences

ISSN: 2710-0758
DOI 10.33886/ajpas.v4i2.412

Journal homepage: http://journal.ku.ac.ke/index.php/AJPAS

Research Article Open Access

# Effect of Absorption and Polarization Potentials in The Distorted Wave Calculation of Positron Impact Excitation of Autoionizing State of Rubidium

**Zakayo Kitui Opungu , Peter Kinuthia Kariuki and Chandra Shekhar Singh**

[1] Department of Physics, Kenyatta University, Nairobi, Kenya
Postal address: 344-30106 Turbo, 43844-00100 Nairobi, 43844-00100 Nairobi
E-mail: xkituyi@gmail.com, kariuki.peterkinuthia@ku.ac.ke and singh.chadra@ku.ac.ke

**Received 20th June, 2022/ Accepted 18th May 2023, Published online 17th November 2023**

**How to cite:**
Opungu, Z., Kariuki, P., & Singh, C. (2023). Effect of Absorption and Polarization Potentials in The Distorted Wave Calculation of Positron Impact Excitation of Autoionizing State of Rubidium. *African Journal of Pure and Applied Sciences*, 4(2), 20-26. https://doi.org/10.33886/ajpas.v4i2.412

## ABSTRACT

This study focuses on the scattering of positrons and rubidium atoms. We utilized the distorted wave approach to compute the cross sections and alignment parameter from near excitation threshold up to 1500 eV. Our system employed Clementi and Roetti (1974) multi-zeta Roothan-Hatree-Fock wave. We employed a complex distortion potential comprising static, absorption, and polarization terms to calculate cross sections and the alignment parameter. Our results were compared with other available studies, and we found that including polarization and absorption potentials significantly affected the cross-sections and the alignment parameter, especially at low-impact energies. These two potentials enhanced the accuracy of both the cross-section and alignment parameter results.

**Keywords:** Cross sections, Rubidium, Distorted wave, Scattering

## INTRODUCTION

Atomic collision processes, which involve the scattering of particles such as protons, electrons, positrons, or ions by target, ions, atoms, or molecules, can be studied theoretically or experimentally, as noted by Joachain in 1975. Theoretical approaches typically employ wave functions to represent the target and distorted waves to represent the projectile. At the same time, experimental methods involve scattering a free beam of particles from a target and detecting the dispersed particles within the asymptotic region. One crucial type of collision process is autoionization, where a collision leads to the excitation of an atom or ion to a state that subsequently decays by electron emission. These autoionizing states are crucial in providing information about the structure of a bit, as cross sections depend strongly on the impact energy, as Theodosius (1987) noted.

Theoretical scattering approaches can be grouped into two broad categories: quantal-mechanical and classical. Semi-classical methods are available, such as the Glauber approximation, semi-classical impact parameter, multichannel eikonal treatment and Monte Carlo method. Quantal-mechanical methods are further divided into non-perturbative and perturbative lines. Perturbative means are used, such as the distorted wave series, many-body theory and Born series. Non-perturbative procedures, such as R-matrix, convergent close coupling, and variation methods, are also used. Madison and Bartschat (1996) provide a detailed discussion of these approaches.

Positron scattering is an important research area with applications in various fields, including astrophysics, plasma science, material science, and medical science, as stated by Marucha (2014). Although experimental results are not yet available for positron-rubidium scattering, two theoretical approaches have been proposed using the static distortion potential. This study used a complex distortion potential that includes static, absorption, and polarization

terms to investigate how different potentials impact results and provide data for future comparisons. The distorted wave methodology was used in this work since it is a high-energy estimation approach that has successfully explained numerous excitation processes and provided results that agree with investigational data at intermediate and high-impact energies, as described by William *et al.* (2021).

## THEORY

The procedure of excitation for rubidium atom by a positron is represented by equation (1).

$$e^+ + Rb\left[np^6(n+1)s\right]^2 S_{\frac{1}{2}} \rightarrow e^+ + Rb^*\left[np^5(n+1)s^2\right]^2 P_{\frac{1}{2}\frac{3}{2}} \quad (1)$$

Equation (2) (Madison and Bartschat, 1996) represents the transition matrix for this excitation process.

$$T_{if} = \left\langle \chi_f^-(r_0)\varphi_f(r_1)\middle|V(r_0,r_1)\middle|\chi_i^+(r_0)\varphi_i(r_1)\right\rangle \quad (2)$$

where $V(r_0, r_1)$ is the interaction potential projectile-target for the atom expressed as;

$$V(r_0,r_1) = \frac{Z_p}{r_0} - \frac{Z_p}{r_{01}} \quad (3)$$

$r_0$ and $r_1$: The position vectors of the atomic electron and the incident positron experiencing transition are measured comparative to the target nucleus, which serves as the source center of the mass for each particle. The vector column $r_{01}$ represents the interval between the target electron and the positron.

$Z_p$ , the incident positron charge taken as $+1$. $\varphi_i$ and $\varphi_f$ are suitably anti-symmetrized starting and ultimate function of the atomic wave for the target atom as obtained from tables presented by Clementi and Roetti (1974).

$\chi_i$ and $\chi_f$ are the disseminated positron slanted functions of the wave in the preliminary and concluding frequencies, correspondingly, with $k_i$ and $k_f$ wave vectors.

The distorted wave expressions were found by unravelling equations (4) and (5).

$$\left(\frac{1}{2}\nabla_0^2 - U_i + \frac{1}{2}k_i^2\right)\chi_i^+ = 0 \quad (4)$$

$$\left(\frac{1}{2}\nabla_0^2 - U_f + \frac{1}{2}k_f^2\right)\chi_f^- = 0 \quad (5)$$

$(+)$ and $(-)$ indicate the outbound and inbound wave border settings, respectively. $U_i$ and $U_f$ are the distorting potentials in the initial and final states, correspondingly.

In evaluating the scattering amplitude provided by the second equation (2), the distorted waves $\chi_f^-$ are first extended in partial waves as follows (Madison and Bartschat, 1996).

$$\left|\chi_i^+\right\rangle = \sqrt{\frac{2}{\pi}}\frac{1}{k_i r}\sum_{l_i m_i} i^{l_i}\chi_{l_i}(k_i,r)Y_{l_i m_i}(\hat{r})Y^*_{l_i m_i}(\hat{k}_i) \quad (6)$$

$$\left|\chi_f^-\right\rangle = \sqrt{\frac{2}{\pi}}\frac{1}{k_f r}\sum_{l_f m_f} i^{l_f}\chi^*_{l_f}(k_f,r)Y_{l_f m_f}(\hat{r})Y^*_{l_f m_f}(\hat{k}_f) \quad (7)$$

where $Y_{lm}$ represents a spherical harmonic.

In expanding $\chi_f^-$ equation (7), the complex combination of radial distorted wave was taken to satisfy the conditions for the incoming wave limit.

The distorted radial waves are results of the differential equation(8):

$$\left(\frac{d^2}{dr^2} - \frac{l_s(l_s+1)}{r^2} - U_s(r) + k_s^2\right)\chi_{ls}(r) = 0 \quad (8)$$

where $s = i$ the initial state and $s = f$ the final state of distorted waves.

Equation (8) was solved using the Numerov method.

### Distortion potentials

The distortion potential used in this study is multifaceted in both channels and expressed by equation (9).

$$U_{if} = V_{i,f}^{st}(r) + V^{abs}(r) + V^{pol}(r) \quad (9)$$

$V_{i,f}^{st}(r)$ represents the static potential, $V^{abs}(r)$ absorption potential, and $V^{pol}(r)$ polarization potential. The static potential adopted for this study is the one used by Nahar and Wadehra (1986) written as;

$$V^{st}(r_0) = \frac{Ze_p}{r_0} - \sum_{i=1}^{Z} e_p \int \left|\Psi(r_1,r_2,...,r_Z)\right| \times \frac{1}{\left|r_0 - r_i\right|} dr_1 ... dr_Z \quad (10)$$

$Z$ represents the target atom nuclear charge while $e_p$ represents the charge of the projectile. $\Psi(r_1,r_2,...,r_Z)$ represents the Hartree-Fock anti-symmetrized wave expression of the target and is lengthened in relation to slater-type orbitals:

$$\Phi_{\lambda p} = \sum_{i=1}^{M} A(\lambda,p,i) r^{n(p,i)-1} \exp\left[-\zeta(p,i)r\right] Y_l^m(\$) \quad (11)$$

where

$$A(\lambda,p,i) = C(\lambda,p,i)\left\{2\left[n(p,i)\right]!\right\}^{-1/2}\left[2\zeta(p,i)\right]^{n(p,i)+1/2} \quad (12)$$

In equation (12);

$C(\lambda, p, i)$ represents the orbital expansion co-efficient.

$\zeta(p,i)$ , the orbital exponent of the Multi-zeta function and

$n(p,i)$ , the principal quantum number.

Clementi and Roetti (1974) tables were used to obtain values of the constants in equation (12)

The study's absorption potential is the one used by Staszewska *et al.* (1984). For the impact energy $E$ at a point $r$ , it is given by:

$$V^{abs}\left(\mathbf{r}, E\right) = -\frac{1}{2} T_{loc} \rho(r) \overline{\sigma_b} \tag{13}$$

where $T_{loc}\left(\mathbf{r}, E\right) = \left[2\left(E - V^s\right)\right]^{1/2}$

$T_{loc}$ , is the incident positron's speed, $V^s$ the static potential, $\rho(r)$ the target atom's electron charge density, and $\overline{\sigma_b}$ the mean binary collision cross-section resulting from the standard Rutherford cross-sections over the density of a free electron gas $\rho(r)$ which is dependent to the restraints

$$\begin{aligned} \left(k'\right)^2 &\geq \alpha \\ \left(p'\right)^2 &\geq \beta \end{aligned} \tag{14}$$

In case of $p'$ and $k'$ are the final momentum of projectile particle and the target electron after a collision.

Nahar and Wadehra (1986) used polarization potential $V^{pol}(r)$, which is represented by the equation;

$$V^{pol}(r) = -\frac{1}{2}\alpha_d^2 / \left(r^2 + d^2\right)^3 \tag{15}$$

in which $\alpha_d = 319$ are the polarizability of the dipole, $d$ the energy-dependent adjustable parameter, and $r$ the orbital radius of the rubidium atom, Reid and Wadehra(1998).

### Cross sections

Differential cross sections have been calculated using equation (16) where the symbols have their usual meanings.

$$\left(\frac{d\sigma}{d\Omega}\right)_{4p\to 5s} = \frac{1}{4\pi^2}\frac{k_f}{k_i}\sum_{m=-1}^{1}\left(\left|T_{4p\to 5s}\right|^2\right) \tag{16}$$

Integral cross sections have been calculated using equation (17) where the symbols have their usual meanings.

$$\sigma = \int_0^{2\pi}\int_0^{\pi}\frac{d\sigma}{d\Omega}\sin\theta d\theta d\phi \tag{17}$$

### Alignment parameter

The alignment parameter $A_{20}$ (Kaur and Srivastava, 1999) is calculated using equation (22).

$$A_{20} = \frac{\sigma(np_1) - \sigma(np_0)}{\sigma(np_0) + 2\sigma(np_1)} \tag{18}$$

where $np_m$ is the whole cross-section of an $np_m$ electron excited to a $(n+1)s$ state.

## RESULTS AND DISCUSSION

This section discusses the results obtained from analyzing positron-rubidium scattering using a complex potential. Specifically, we present the results of the differential cross sections, alignment parameter, and integral cross sections. In our analysis, we considered various types of distortion potentials, including static potential only, dormant potential with absorption potential, static potential with polarization probable, and static potential with absorption and polarization potential. To assess the validity of our results, we compared them with theoretical results obtained by Marucha (2014) and with experimental results obtained by Pangantiwar and Srivastava (1987).

### Integral cross-sections

This segment compares our integral cross-section results for positron-rubidium scattering with those reported by Pangantiwar and Srivastava (1987) and Marucha (2014). We found that when using static potential only, our integral cross-section results were qualitatively similar to those obtained by Marucha, Pangantiwar, and Srivastava, as illustrated in figure 1. However, the difference in magnitude is attributed to the method used to evaluate the static potential. In particular, our current static potential was evaluated numerically, whereas the previous static possibilities were assessed analytically. When absorption potential was included in our analysis, we observed a decrease in the degree of the integral cross sections at low-impact energies. This decrease is attributed to the absorption potential's ability to account for transitions to other channels.

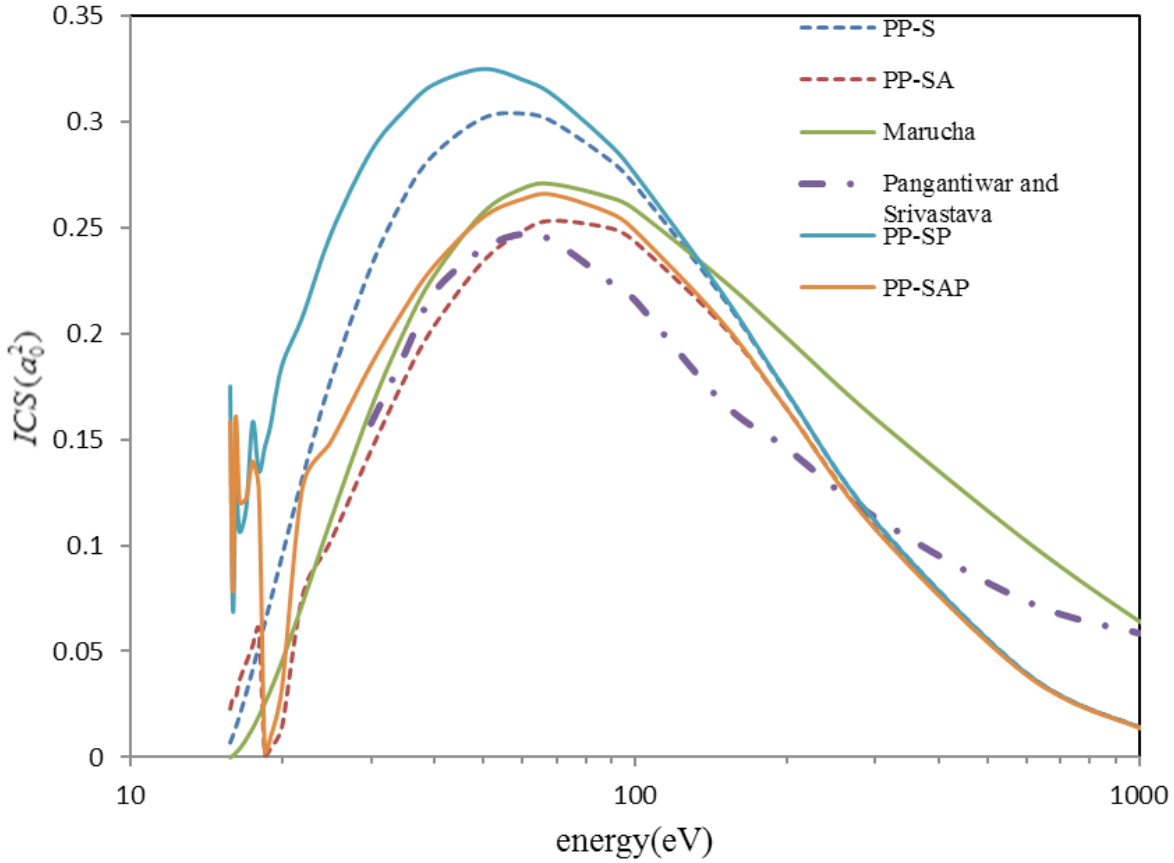


**Figure 1.** Integral cross-section results for the positron-induced excitation of the autoionizing state of rubidium are presented. We compare the present results obtained using different types of potentials: PP-S, which represents the results obtained using static potential only; PP-SA, which means the results obtained using dormant and absorption potentials; PP-SP, which represents the results obtained using static and polarization potentials; and PP-SAP, which represents the results obtained using static, absorption, and polarization potentials.

In addition to our present results, we also compare our findings with those reported by Marucha (2014) and Pangantiwar and Srivastava (1987), who investigated positron-induced excitation of the autoionizing state of rubidium.

The absorption potential exhibits little impact on the cross sections' integral at high impact energies because the short interaction time between the target and the fast-moving projectile limits its observable effects (Marucha, 2014). Thus, the absorption potential's impact is negligible at such energies. On the other hand, the polarization potential introduces a resonance edifice near the excitation threshold when used in conjunction with the static prospect. This resonance structure signifies that the probability of scattering is higher near the excitation threshold, resulting in a higher degree of integral cross-sections at energies that are at low-impact. The polarization potential's impact is due to its ability to handle target polarization (Marucha, 2014).

Even when all three potentials are used, the resonance construction close to the excitation threshold persists, as observed in Marucha's (2014) study. However, at high impact energies, neither the absorption nor the polarization potential exhibits an observable effect on the integral cross sections due to the projectile's short interaction time with the target. Therefore, even with all three possibilities included, the noticeable results are limited at high-impact energies (Marucha, 2014).

## Differential cross-sections

A juxtaposition was conducted between the differential cross-section outcomes for positron-rubidium scattering obtained at different impact energies (20, 30, 50, 100, and 200 eV) in this study and those reported by Marucha (2014). The present results, which utilized the static potential exclusively, exhibit qualitative agreement with Marucha's findings, as shown in figure 2 (a). The observed differences in magnitude are attributed to the selection and methodology employed in evaluating the static potential. Marucha used analytical methods to determine the fixed potential, while the present study utilized numerical methods.

When the absorption potential is incorporated, it reduces the magnitude of the differential cross-sections by accounting for transitions to channels

that are irrelevant to this study. Consequently, the cross-section magnitude decreases. Conversely, the polarization potential increases the differential cross-section magnitude by accounting for the target's polarization. In figure 2 (b), using static potential exclusively, the current differential cross sections demonstrate the same trend as Marucha's results. The absorption potential diminishes the differential cross-section magnitude, while the polarization potential boosts the cross-section magnitude.

As the potentials are combined, the graphs for static potential only, static potential + absorption potential, static potential + polarization potential, and static potential + absorption + polarization potential converge.

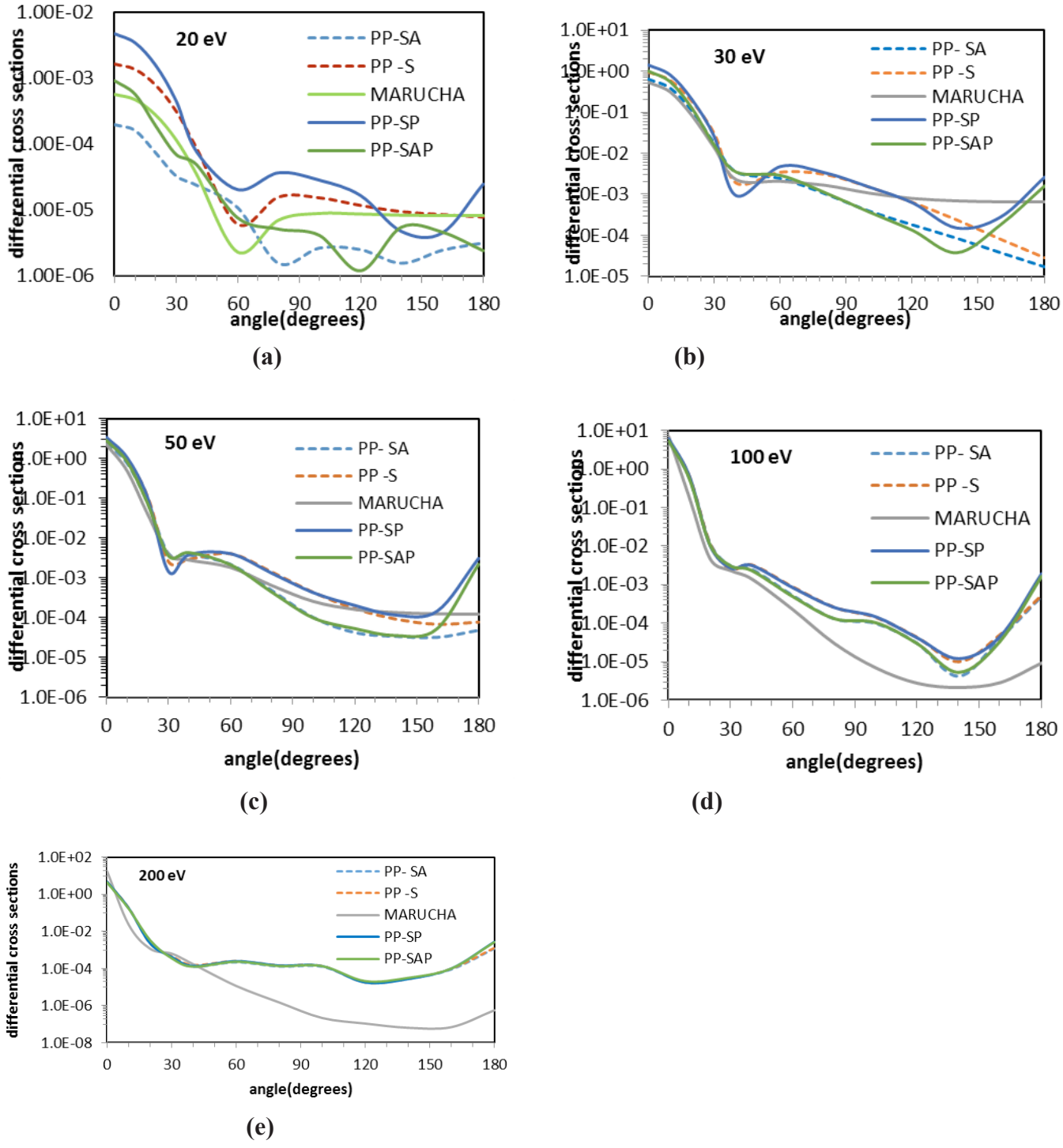


**Figure 2.** Differential cross sections for positron-rubidium at (a) 20 eV, (b) 30 eV, (c) 50 eV, (d) 100 eV, and (e) 200 eV PP-SA; Present results with absorption and polarization potential, PP-S; Present results with static potential only, Marucha; Results by Marucha 2014, Pangantiwar and Srivastava; Results by Pangantiwar and Srivastava 1987, PP-SP; Present results with static and polarization potential, PP-SAP; Present results with static, absorption and polarization potentials.

In this work, the differential cross sections obtained for impact energies oscillating from 20 eV to 200 eV were compared with the results presented by Marucha (2014), as illustrated in figure 2. The comparison revealed that the qualitative connection between the outcome obtained using only the static potential and those obtained by Marucha(2014) is good, as depicted in figure 2(c). The discrepancy in the results magnitudes can be attributed to the numerical evaluation of the current static potential instead of the analytical assessment employed by Marucha(2014).

Furthermore, the effects of including absorption and polarization potential on the differential cross-sections were investigated. It was observed from the graphs in figure 2(d) that the inclusion of these potentials decreased their effects on the differential cross-sections. The results showed a slight difference in magnitudes between the cross sections with and without these potentials, suggesting a negligible effect.

At higher impact energies, as illustrated in figure 2(e), the graphs for the cross sections obtained using static potential only, static potential + absorption potential, static potential + polarization potential, and static potential + absorption + polarization potential converge entirely. This convergence is because the projectile moves at high speed at high energies, resulting in a short interaction time with the target. Therefore, the effects of absorption and polarization potential on the differential cross sections are minimal, as William *et al.* (2021) reported.

## Alignment parameter

Determining the alignment parameter is critical in evaluating the ratio of integral cross sections, as it offers additional insights into the distribution of magnetic sub-states. In this study, we compared the alignment parameter outcomes with those obtained by Marucha (2014) and Pangantiwar and Srivastava (1987), as illustrated in figure 2. Our results employ only static potential and exhibit a similar trend to Pangantiwar, Srivastava, and Marucha's findings. However, there is a discrepancy in magnitude, which can be attributed to the selection and assessment of the static potential.

Furthermore, our study incorporates the absorption potential, having a noticeable impact on the outcomes at low-impact energies, as depicted in figure 3. This energy range accentuates the absorption potential's considerable influence on the results, a factor that is absent at higher energies, as indicated by William *et al.* (2021).

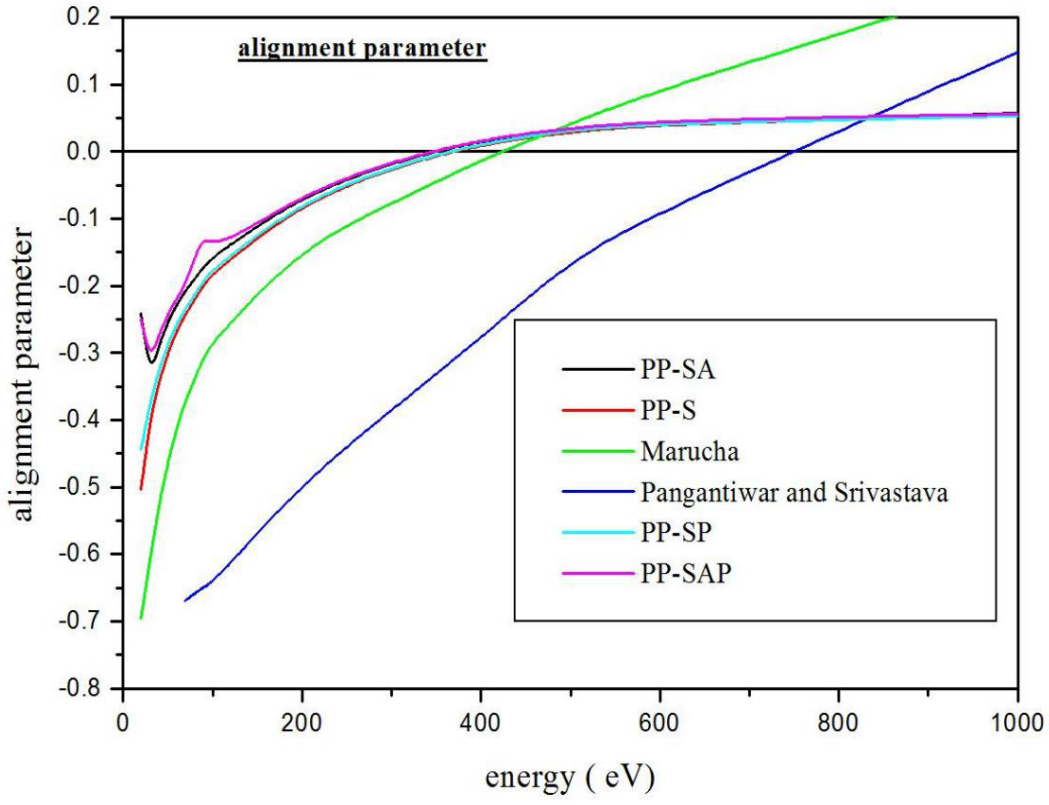


**Figure 3.** Alignment parameter results. PP-SA; Present results with absorption and polarization potential, PP-S; Present results with static potential only, Marucha; Results by Marucha 2014, Pangantiwar and Srivastava; Results by Pangantiwar and Srivastava 1987, PP-SP; Present results with dormant and polarization potential, PP-SAP; Present results with static, absorption and polarization prospects.

According to William *et al*. (2021), the integral cross sections at intermediate energies decrease as the projectile travels through the target with minimal interaction, lessening time of collision and interaction probability. The polarization potential introduces a resonance design near the excitation threshold. The results of all three possibilities follow the same trend as those obtained with the static potential alone. At high-impact energies, the effects of the absorption and polarization possibilities become insignificant due to the short interaction time, which is not sufficient for the possibilities to manifest.

Moreover, the alignment parameter is negative when the impact energies are below 400 eV. This parameter is a ratio of integral cross-sections that provides information on the number of magnetic sub-states. The negative value indicates that the magnetic sub-states with lower angular momentum are more populated than those with higher ones. This observation is consistent with the findings of previous studies by Marucha (2014) and Pangantiwar and Srivastava (1987).

The formula for calculating the alignment parameter suggests that it can only be negative if a specific condition is met. Marucha (2014) found that the magnetic sub-state dominates the excitation process compared to the magnetic sub-state. The negative alignment parameter observed for impact energies less than 400 eV indicates that the former sub-state is more populated. However, the alignment parameter for impact energies above 400 eV becomes positive, indicating that the excitation primarily occurs from the magnetic sub-state m = 1.

## CONCLUSION

Utilizing the distorted wave method, this work investigated positron-rubidium scattering cross-sections and alignment parameters across a range of impact energies from near excitation threshold up to 1500 eV. The results of this investigation are compared with the Pangantiwar and Srivastava (1987) and Marucha (2014) theoretical approaches. The present results agree with the two theoretical models when only static potential is used. However, at low-impact energies, including absorption potential decreases the extent of both differential and integral cross sections, whereas the incorporation of polarization potential increases their magnitudes. Nevertheless, the two prospects have minimal effects at high-impact energies as a result of the brief interaction time between the target and the projectile. Considering the inclusion of both polarization and absorption potentials, the present study's results are expected to be more precise than the previous theoretical models. Additionally, future experimental outcomes are anticipated to align well with the current findings.

## REFERENCES


Clementi E. and Roetti C. (1974). Roothan—Hartree -Fock Atomic Wave functions. *Atomic Data Nuclear Data Tables* 14:177–478

Joachain, C. J. (1975).*Quantum Collision Theory*. North Holland Publishing Company, Amsterdam.

Kaur, S. and Srivastava, R. (1999). Excitation of the lowest autoionizing states of Na (n = 2),K(n=3), Rb (n = 4) and Cs (n = 5) by electron impact. *Journal of Physics B: Atomic, Molecular and Optical Physics* 32:2323–2342

Madison H. and Bartschat K. (1996). The distorted wave method for elastic Scattering and atomic excitation. In : *Computational Atomic Physics. E*d. K Bartschat. (Berlin: Springer) Pg 65–85

Marucha A. (2014) Positron impact excitation of the lowest autoionizing state in rubidium atom using distorted wave method. *Scholars Journal of Physics, Mathematics and Statistics* 2014; 1(2):118-125

Nahar, S. N. and Wadehra, J. M. (1986). Elastic Scattering of positrons and electrons by argon. *Physical Review A* 35 5

Pangantiwar, A. and Srivastava, R. (1987). $e^{\pm}e^{\pm}$ impact excitation of autoionizing levels in alkalis: a distorted wave approach. *Journal of Physics B : Atomic, Molecular and Optical Physics* 20: 5881-5902

Reid, D. and Wadehra, J. (1998). Intermediate- to high-energy positrons scattered by alkali-metal atoms. *Physical Review A* 57: 2583–2589

Staszewska, G. Schwenke, D. W. and Truhlar, D. G. (1984). Investigation of the shape of the imaginary part of the optical-model potential for electron scattering by rare gases. *Physical Review A* 29:6

Theodosious E. (1987) Collisional excitation and alignment of $np^5(n+1)s^2np^5(n+1)s^2$ autoionizing states of the alkali-metal atoms. *Physical Review A* 36: 3139-3145

William, N. Jobunga, E. and Singh, C.(2021). Positron impact excitation of lowest autoionizing state of potassium atom using distorted wave method with absorption and polarization potentials. *Journal of Physics and Communications 5* (2021) 025006 https://doi.org/10.1088/2399-6528/abe035